

DEEP OPTICAL IMAGING OF A COMPACT GROUP OF GALAXIES, SEYFERT'S SEXTET

SHINGO NISHIURA^{1,2}, TAKASHI MURAYAMA^{1,2,3}, MASASHI SHIMADA^{1,2,4}, YASUNORI SATO^{3,5}, TOHRU NAGAO^{1,3}, KOHJI MOLIKAWA¹, YOSHIAKI TANIGUCHI^{1,2,3}, AND D. B. SANDERS⁶

¹Astronomical Institute, Graduate School of Science, Tohoku University, Aramaki, Aoba, Sendai 980-8578, Japan

²Visiting astronomer of Okayama Astrophysical Observatory, National Astronomical Observatory of Japan

³Visiting astronomer of Mauna Kea Observatories, University of Hawaii

⁴Asahi Optical Co., Ltd. Optical Research Department, 2-36-9, Maeno-cho, Itabashi-ku, Tokyo, 174-8639, Japan

⁵ISAS, 3-1-1 Yoshinodai, Sagami-hara, Kanagawa 229-8510, Japan

⁶Institute for Astronomy, University of Hawaii, 2680 Woodlawn Drive, Honolulu, HI 96822

THE ASTRONOMICAL JOURNAL, 120, No. 5 in press.

ABSTRACT

In order to investigate the dynamical status of Seyfert's Sextet (SS), we have obtained a deep optical ($VR + I$) image of this group. Our image shows that a faint envelope, down to a surface brightness $\mu_{\text{optical}}(\text{AB}) \simeq 27 \text{ mag arcsec}^{-2}$, surrounds the member galaxies. This envelope is irregular in shape. It is likely that this shape is attributed either to recent-past or to on-going galaxy interactions in SS. If the member galaxies have experienced a number of mutual interactions over a long timescale, the shape of the envelope should be rounder. Therefore, the irregular-shaped morphology suggests that SS is in an early phase of dynamical interaction among the member galaxies. It is interesting to note that the soft X-ray image obtained with ROSAT (Pildis et al. 1995) is significantly similar in morphology. We discuss the possible future evolution of SS briefly.

Subject headings: galaxies: group: individual (Seyfert's Sextet = HCG 79) - dark matter: galaxies - X-rays: galaxies

1. INTRODUCTION

Since groups of galaxies are intermediate in number density between isolated galaxies and rich clusters of galaxies, it is important to investigate their dynamical properties in detail. Recently, the X-ray satellite ROSAT has been used to investigate the dark matter content of a large number of groups of galaxies because the hot gas probed in soft X-rays is generally believed to be gravitationally bound to the groups (Ponman & Bertram 1993; Ebeling, Voges, & Böhringer 1994; Pildis, Bregman, & Evrard 1995; Saracco & Ciliegi 1995; Ponman et al. 1996; Mulchaey & Zabludoff 1998). As expected, the majority of groups of galaxies detected by ROSAT show round-shaped morphologies in the soft X-ray. On the other hand, a few groups such as Seyfert's Sextet (hereafter SS), show irregular-shaped soft X-ray morphologies (Pildis et al. 1995). The X-ray morphology can provide important information about the dynamical status of groups of galaxies. Another useful method to investigate the dynamical status is to search for a faint optical envelope surrounding a group of galaxies (Nishiura 1998). In this paper, in order to investigate the dynamical status of SS, we present a very deep optical image of this group and compare it with the soft X-ray halo obtained by Pildis et al. (1995).

SS is one of the most famous as well as densest compact group of galaxies (Seyfert 1948a, 1948b). This group is also a Hickson Compact Group of Galaxies, HCG 79 (Hickson 1982, 1993). The basic data of the galaxies in SS are listed in Table 1 taken from Hickson (1993). SS consists of four redshift-accordant galaxies (HCG79a,

HCG79b, HCG79c, and HCG79d). Note that HCG 79e is a redshift-discordant galaxy which is believed to have no physical relation to SS. Also, the NE optical fuzz is now considered to be tidal debris associated with HCG 79b (Rubin, Hunter, & Ford 1991; Williams, McMahon, & van Gorkom 1991; Mendes de Oliveira & Hickson 1994; Vilchez & Iglesias-Páramo 1998). We assume a distance to SS of $44h^{-1}$ Mpc determined using the mean recession velocity of HCG 79a, HCG 79b, HCG 79c, and HCG 79d referenced to the galactic standard of rest, $V_{\text{GSR}} = 4449 \text{ km s}^{-1}$ (de Vaucouleurs et al. 1991), and a Hubble constant, $H_0 = 100 h \text{ km s}^{-1} \text{ Mpc}^{-1}$.

2. OBSERVATIONS

2.1. Optical Imaging

Optical VR - and I -band deep images of SS were obtained with the 8192×8192 (8K) CCD mosaic camera (Luppino et al. 1996) attached to the f/10 Cassegrain focus of the University of Hawaii 2.2 m telescope at Mauna Kea Observatory, on 20 May 1999 (VR) and 23 May 1999 (I). The camera provided a $\sim 18' \times 18'$ field of view. Two-pixel binning was used yielding a spatial resolution of 0.26 arcsec per element. The integration time for each exposure was set to 8 minutes. Twenty-three exposures for the VR -band and 24 exposures for the I -band were taken; thus, the total integration time amounted to 10,560 seconds in the VR -band image and 11,520 seconds in the I -band image. The seeing was ~ 0.8 arcsec during the observation.

Data reduction was performed in a standard way using IRAF¹. Flux calibration was made using the data of

¹Image Reduction and Analysis Facility (IRAF) is distributed by the National Optical Astronomy Observatories, which are operated by the

TABLE 1
 PROPERTIES OF THE MEMBER GALAXIES OF SS AND THE DISCORDANT GALAXY HCG 79E

Name	Type	V_{GSR} (km s^{-1})	B_{T}^0 (mag.)	L_{B} ($h^{-2} \text{ ergs s}^{-1}$)	$L_{\text{X,exp}}$ ($h^{-2} \text{ ergs s}^{-1}$)
HCG 79a	E0	4395	14.35	43.32	38.86
HCG 79b	S0	4547	13.78	43.55	39.43
HCG 79c	S0	4247	14.72	43.18	38.50
HCG 79d	Sdm	4604	15.87	42.72	38.50
HCG 79e	Scd	19910	15.87	44.03	40.09

photometric standard stars in the field of SA 103, SA 104, SA 107, SA 109, and SA 110 (Landolt 1992). Since the VR -band is not a standard photometric band (Jewitt, Luu & Chen 1996), we adopted an AB magnitude scale for this bandpass. The photometric errors were estimated to be ± 0.05 mag for the VR -band and ± 0.03 mag for the I -band. The limiting surface brightnesses are $\mu_{VR}^{\text{lim}} = 28.7$ mag arcsec $^{-2}$ and $\mu_I^{\text{lim}} = 28.1$ mag arcsec $^{-2}$, corresponding to a 1σ variation in the background. The VR , I , and $VR + I$ images are shown in Figure 1 (a), Figure 2 (a), and Figure 3, respectively.

FIG. 1.— (a) VR image of SS. Black contours are drawn above $\mu_{AB} = 27$ mag arcsec $^{-2}$ with an interval of 1 mag arcsec $^{-2}$. (b) Images of model galaxies of SS in VR -band. And, (c) Model subtracted image of SS in VR -band. The horizontal bars correspond to 1 arcmin $\simeq 12.8 h^{-1}$ kpc. North is up and east is to the left.

FIG. 2.— (a) I image of SS. Black contours are drawn above $\mu_I = 27$ mag arcsec $^{-2}$ with an interval of 1 mag arcsec $^{-2}$. (b) Images of model galaxies of SS in I -band. And, (c) Model subtracted image of SS in I -band. The horizontal bars correspond to 1 arcmin $\simeq 12.8 h^{-1}$ kpc. North is up and east is to the left.

2.2. Optical Spectroscopy

In order to investigate the nuclear activity of the member galaxies of SS, we have performed optical spectroscopy during the course of our optical spectroscopy program of Hickson compact groups of galaxies (Shimada et al. 2000; Nishiura et al. 2000). Optical spectra were obtained with the Cassegrain spectrograph attached to the 188 cm telescope at the Okayama Astrophysical Observatory (OAO) on 22 February (HCG 79a), 15 August (HCG 79b), and 18 August 1996 (HCG 79c and HCG 79d). A 600 lines/mm grating blazed at 7,500 Å was used. The spectral coverage was 6,200 Å – 6,900 Å with a spectral resolution of 2.4 Å at 6,500 Å. The integration time was 1800 seconds for each galaxy. The spatial resolution was 1.75 arcsec pixel $^{-1}$ and the slit width was 1.8 arcsec. The seeing size was 2 arcsec during the observations. The data reduction was made using IRAF with a special package SNGRED for the OAO spectrograph (Kosugi et al. 1995). Spectroscopic standard stars (HD 84937, HD 161817, HD 217086, BD 322642, and Feige 15) were observed to calibrate the spectra. One-dimensional nuclear spectra of the four member

galaxies were extracted by tracing the central two pixels; i.e., 3.5 arcsec. The final nuclear spectra are shown in Figure 4.

FIG. 3.— (a) I image of SS. Black contours are drawn above $\mu_I = 27$ mag arcsec $^{-2}$ with an interval of 1 mag arcsec $^{-2}$. (b) Images of model galaxies of SS in I -band. And, (c) Model subtracted image of SS in I -band. The horizontal bars correspond to 1 arcmin $\simeq 12.8 h^{-1}$ kpc. North is up and east is to the left.

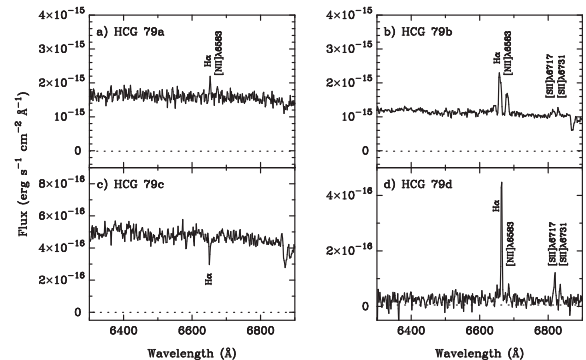


FIG. 4.— Optical spectra of a) HCG 79a, b) HCG 79b, c) HCG 79c, and d) HCG 79d.

3. RESULTS AND DISCUSSION

3.1. The Morphology of the Faint Optical Envelope

As shown in Figure 1 (a), Figure 2 (a), and Figure 3, we can see a faint optical envelope surrounding SS both in the VR image and in the I image. However, since the member galaxies are very close together on the sky, we cannot rule out a possibility that we may misidentify the overlapping isophotes of galaxies for the real faint optical envelope. In order to confirm the presence of the faint optical envelope, it is necessary to subtract off models of all the galaxies in SS. For this purpose we have made a model of each galaxy in SS by fitting a surface brightness profile of its outer region. In this procedure, we adopt a de Vaucouleurs' $r^{1/4}$ law for HCG 79a and 79c and an exponential law for HCG 79b, 79d, 79e. We also made a model for the tidal debris east of HCG 79b (see Fig. 3) with an exponential law. Surface photometry was carried out using the Surface Photometry Interactive Reduction and Analysis Library (Hamabe & Ichikawa 1992). We made an image of the model SS by adding the above models. In this

TABLE 2
PARAMETER OF MODEL GALAXIES

Name	band	radius (arcsec)	mag.	profile ^a	ellipticity	P.A. (degree)
HCG 79a	<i>VR</i>	7.98	13.09	$r^{1/4}$	0.30	158.0
	<i>I</i>	7.72	12.30	$r^{1/4}$	0.30	158.0
HCG 79b	<i>VR</i>	3.42	12.92	exp	0.67	177.0
	<i>I</i>	3.24	12.65	exp	0.65	174.0
HCG 79c	<i>VR</i>	2.59	13.65	$r^{1/4}$	0.52	126.0
	<i>I</i>	3.46	12.99	$r^{1/4}$	0.52	126.0
HCG 79d	<i>VR</i>	8.09	15.80	exp	0.74	87.0
	<i>I</i>	8.48	15.11	exp	0.77	86.0
HCG 79e	<i>VR</i>	3.90	15.24	exp	0.06	54.0
	<i>I</i>	3.84	14.55	exp	0.06	58.0
Tidal debris	<i>VR</i>	6.35	17.24	exp	0.88	133.4
	<i>I</i>	6.09	16.49	exp	0.90	133.4

^a $r^{1/4}$ means de Vaucouleurs' $r^{1/4}$ law and exp means exponential law.

procedure we use the ARTDATA package with the fitting parameters derived by the surface photometry. In Table 2 we list the parameters of our model galaxies. For the model of the tidal debris east of HCG 79b, it seems that there is a much better fit would be found with a rounder model at a larger position angle. Fainter parts of the debris may be connected to the optical envelope. Therefore, we have made our model fit for the brighter part of the debris and then subtracted it from the image.

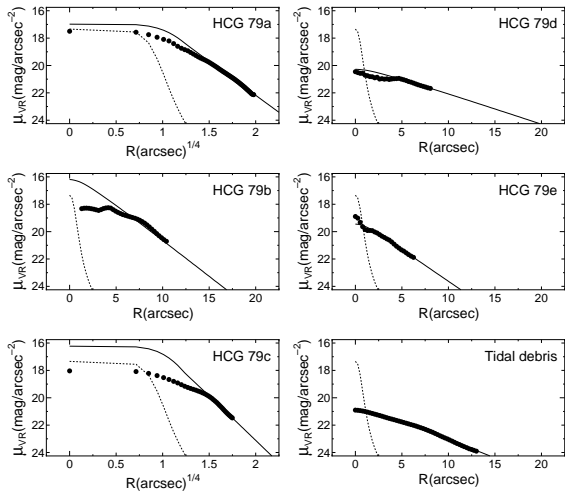


FIG. 5.— *VR*-band surface brightness profiles along the major axis of the galaxies in SS. The filled circles indicate the profiles of observed galaxies. The solid lines indicate the profiles of model galaxies. The dotted lines indicate the profiles of a star observed in the same frame.

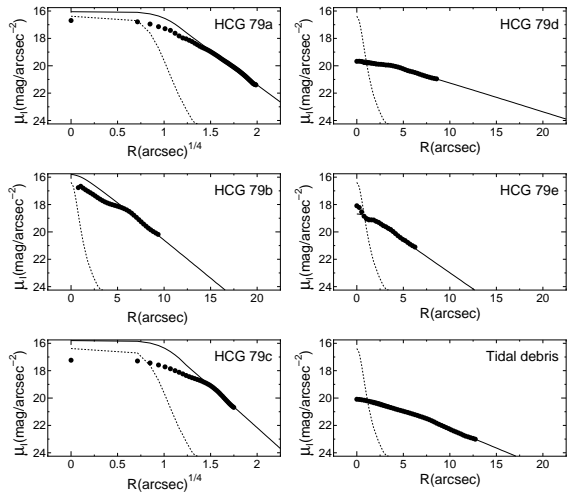


FIG. 6.— *I*-band surface brightness profiles along the major axis of galaxies in SS. The filled circles indicate the profiles of observed galaxies. The solid lines indicate the profiles of model galaxies. The dotted lines indicate the profiles of a star observed in the same frame.

The results are shown in Figure 1 (b) (*VR*-band) and 2 (b) (*I*-band). The model subtracted images are shown in Figure 1 (c) (*VR*-band) and 2 (c) (*I*-band). Figure 5 and 6 show the *VR*- and *I*-band surface brightness profiles of all the galaxies in SS. The filled circles indicate the observed profiles and solid lines indicate the profiles of the model galaxies. As a result of the model subtraction, we can still see the faint optical envelope surrounding SS both in the *VR* image and in the *I* image.

Next, in order to check whether the skirts of the point spread function (PSF) of the galactic nuclei contaminate the faint optical envelope, we compared the surface brightness profiles of all the galaxies in SS with that of a star in the same frame of SS. The surface brightness profile of the star is shown as dotted lines in Figure 5 and 6. We

TABLE 3
EMISSION-LINE PROPERTIES OF THE MEMBER GALAXIES OF SS

Name	$\log f_{H\alpha}$ (ergs s ⁻¹ cm ⁻²)	[N II] λ 6583/H α	[S II] λ 6583/H α	FWHM(H α) (km s ⁻¹)	EW(H α) (\AA)
HCG 79a	-14.60 ± 0.09	0.52 ± 0.19	...	150 ± 37	$-1.13^{+0.21}_{-0.26}$
HCG 79b	-14.00 ± 0.02	0.53 ± 0.04	0.27 ± 0.03	337 ± 14	$-6.76^{+0.30}_{-0.31}$
HCG 79c	absorption
HCG 79d	-14.75 ± 0.02	0.12 ± 0.02	0.44 ± 0.06	121 ± 7	-116 ± 5

cannot find any contribution of the light of the PSF to the faint optical envelope surrounding SS both in the VR image and in the I image. Throughout these two checks we have confirmed that the faint optical envelope is really present around SS.

Using the images in Figure 1c and Figure 2c, we roughly calculate the VR and I magnitudes of the faint optical envelope by integrating the light without any point sources (i.e., stars in our Galaxy) within a circle of the centered at $\alpha = 15^{\text{h}}56^{\text{m}}59^{\text{s}}.6$, and $\delta = +20^{\text{d}}54^{\text{m}}59^{\text{s}}.6$ with a radius of 70 arcsec enclosing the optical faint envelope of SS. The regions which appear black on Figure 1c and 2c are also ignored. We obtain $VR_{\text{AB}} \simeq 14.5$ and $I \simeq 13.7$ for the envelope. The luminosity contribution of the envelope to the total luminosity is $\approx 12\%$ in VR and $\approx 13\%$ in I . This implies that the envelope consists of red stars. If we assume that the mass-to-light ratio of the stellar component of the optical faint envelope is $M/L = 3.57 \pm 0.43$ (M_{\odot}/L_{\odot}) in I -band (Worthey 1994), we obtain the mass of the optical faint envelope, $M_{\text{env}} \simeq (9.1 \pm 1.1) \times 10^9 M_{\odot}$.

The morphology of the faint optical envelope in the VR image is quite similar to that in the I image. The overall morphology of the individual galaxies is consistent with that obtained previously (Sulentic & Lorre 1983). The faint optical envelope shows an irregular shape. It is likely that this shape is attributed either to recent-past or to on-going galaxy interactions in SS. If the member galaxies have experienced a number of mutual interaction over a long timescale, the shape of the envelope might reasonably be expected to be rounder. Therefore, the irregular-shaped morphology suggests that SS is in an early phase of dynamical interactions among the member galaxies.

Rubin et al. (1991) and Nishiura et al. (2000) showed that the optical rotation curve of HCG 79d is peculiar compared to those of normal spirals. Williams et al. (1991) obtained an H I map of SS and found that the H I emission, whose intensity peak appears at the center of HCG 79d, shows a southern extension from HCG 79d. They interpreted this as possible evidence for the interaction between HCG 79d and 79b. It is thus strongly suggested that HCG 79d shows tidal effects from this interaction.

Finally, we compare our very deep optical image [$VR+I$; Figure 3] with the soft X-ray image taken by Pildis et al. (1995) in Figure 7. It is shown that the soft X-ray morphology is quite similar to that seen in the optical. The optical faint envelope is most likely attributed to stars liberated from the member galaxies through past and on-going tidal interactions. Therefore, the morphological similarity between the optical and soft X-ray images implies that the dark matter in SS was originally associated with the individual galaxies and then has been liberated tidally together with the stars.

3.2. The Origin of Soft-X Ray Emission

The total soft X-ray luminosity of SS is given only as an upper limit, $L_{\text{X,tot}} < 1.3 \times 10^{41} h^{-2}$ ergs s⁻¹ with ROSAT PSPC (Ponman et al. 1996; hereafter P96). On the other hand, using the same data, Pildis et al. (1995) detected soft X-ray photons at the 2.6σ level. The net count of the extended soft X-ray emission was 28.4 ± 11.1 during the total integration time of 4910 sec. Using the software Xspec², we estimate the soft X-ray luminosity of the extended emission; $L_{\text{X}} \sim 1.3 \times 10^{40} h^{-2}$ ergs s⁻¹ for $kT = 0.5$ keV or $L_{\text{X}} \sim 1.4 \times 10^{40} h^{-2}$ ergs s⁻¹ for $kT = 1$ keV, where the metal abundances are assumed to be 0.3 times solar. It is difficult to resolve X-ray emission from individual galaxies using the ROSAT PSPC because of the compactness of SS itself, even if the exposure time were long enough. It is possible that a part of the X-ray emission may be associated with individual member galaxies. Here we also attempt to examine whether or not the soft X-ray emission of SS really arises from hot gas since supernova remnants, low- and high-mass X-ray binaries, and/or active galactic nuclei could also contribute substantially to the soft X-ray emission to some extent if they are present in the member galaxies.

First we estimate the expected soft X-ray luminosities of discrete sources such as X-ray binaries in the individual galaxies $L_{\text{X,gal}}$. Such soft X-ray luminosities can be estimated using the following empirical $L_{\text{X}} - L_{\text{B}}$ relationship for galaxies where L_{B} is the absolute blue luminosity.

$$\log L_{\text{X}} = (2.47 \pm 1.01) \times \log L_{\text{B}} - (68.36 \pm 44.08),$$

for early-type galaxies (Brown & Bregman 1998), and

$$\log L_{\text{X}} = (1.21 \pm 0.03) \times \log L_{\text{B}} - (13.29 \pm 1.39).$$

FIG. 7.— The soft X-ray image (black contours) taken from Pildis et al. (1995) is overlaid on our $(VR+I)$ CCD image. The Soft X-ray contours are drawn at 1σ , 2σ , 4σ , and 8σ above the background level.

²Xspec is available at <http://heasarc.gsfc.nasa.gov/webspec/webspec.html>

for late-type galaxies (Read, Ponman, & Strickland 1997; Vogler, Pietish, & Kahabka 1996). In Table 1, we give a summary of the expected soft X-ray luminosities for the individual galaxies where L_B is estimated using the apparent blue magnitudes (Hickson 1993). Although HCG 79e is the redshift-discordant galaxy, this galaxy also contributes to the observed soft X-ray luminosity of SS because it lies in a line of sight toward the group. We obtain an expected total soft X-ray luminosity coming from individual soft X-ray sources in the five galaxies; $L_{X,\text{gal}} \simeq 4.4 \times 10^{39} h^{-2}$ ergs s^{-1} , which is much lower than the observed soft X-ray luminosity of SS.

Second, we estimate possible contributions of soft X-ray emission from starburst phenomena in the member galaxies, $L_{X,\text{HII}}$. The spectroscopic properties of the member galaxies based on our optical spectra (Figure 4) are summarized in Table 3. Our results show that HCG 79a, 79b and 79d have a weak HII nucleus. HCG 79c shows no emission-line activity. For starburst galaxies, an average soft X-ray to optical B luminosity ratio is estimated as, $\log L_X/L_B \simeq -3.87 \pm 0.19$ (Read et al. 1997). We estimate that the soft X-ray luminosities from an H II nucleus in HCG 79a, 79b and 79d are $L_{X,\text{HII}} = 2.8 \times 10^{39} h^{-2}$, $4.8 \times 10^{39} h^{-2}$, and $7.1 \times 10^{38} h^{-2}$ ergs s^{-1} , respectively. Thus, we obtain a total soft X-ray luminosity from starbursts in these galaxies, $L_{X,\text{HII}} = 8.3 \times 10^{39} h^{-2}$ ergs s^{-1} .

The model estimated total soft X-ray luminosity from SS, which is the sum total we have calculated above for the soft X-ray luminosity of the individual galaxies, is 1.3×10^{40} ergs s^{-1} . This value is nearly identical to our estimated value using Xspec, $L_{X,\text{tot}} = 1.3 \times 10^{40} h^{-2}$ ergs s^{-1} with $kT=0.5\text{keV}$ and $Z=0.3 Z_\odot$ assumed, and $L_{X,\text{tot}} = 1.4 \times 10^{40} h^{-2}$ ergs s^{-1} with $kT=1.0\text{keV}$ and $Z=0.3 Z_\odot$ assumed.

Finally, we estimate the X-ray luminosity of hot gas trapped by the gravitational potential of SS, $L_{X,\text{gas}}$. Mulchaey & Zabludoff (1998) find a correlation between soft X-ray luminosity from hot gas within poor clusters $L_{X,\text{gas}}$ and radial velocity dispersion σ_r of galaxies in them,

$$\log L_X = (31.61 \pm 1.09) + \log h^{-2} + (4.29 \pm 0.37) \times \log \sigma_r.$$

Using this empirical relation, we obtain $L_{X,\text{gas}} = 6.2 \times 10^{40} h^{-2}$ ergs s^{-1} using the observed value $\sigma_r = 138$ km s^{-1} for SS. This value is a factor of five larger than the observed X-ray luminosity. Since the sum total we calculate for the soft X-ray luminosity of the individual galaxies is high enough to explain the observed X-ray luminosity, it is not necessarily to take account of the mass contribution from the hot gas. Deeper X-ray observations of SS are needed to discuss the nature of the hot gas in SS.

3.3. The Dynamical Properties of Seyfert's Sextet

To discuss the dynamical properties of SS, we first estimate the dynamical mass of the system. Heisler, Tremaine & Bahcall (1985) have proposed four mass estimators for small-member galaxy associations such as compact groups of galaxies; 1) the virial mass estimator M_{vir} , 2) the projected mass estimator M_{proj} , 3) the average mass estimator M_{avg} , and 4) the median mass estimator M_{med} . In order to avoid accidental errors in each mass estimator, we estimate the total mass of SS by averaging masses derived

from these four estimators; $M_{\text{tot}} \simeq 3.6 \times 10^{11} h^{-1} M_\odot$. The results are summarized in Table 4.

TABLE 4
PROPERTIES OF SS

Properties	
$L_{X,\text{tot}}$ (P96)	$< 1.3 \times 10^{41} h^{-2}$ ergs s^{-1}
$L_{X,\text{tot}}$ ($kT=0.5$ keV, $Z=0.3Z_\odot$)	$1.3 \times 10^{40} h^{-2}$ ergs s^{-1}
$L_{X,\text{tot}}$ ($kT=1.0$ keV, $Z=0.3Z_\odot$)	$1.4 \times 10^{40} h^{-2}$ ergs s^{-1}
$L_{X,\text{gal}}$	$4.4 \times 10^{39} h^{-2}$ ergs s^{-1}
$L_{X,\text{HII}}$	$8.3 \times 10^{39} h^{-2}$ ergs s^{-1}
$L_{X,\text{gas}}$	$6.2 \times 10^{40} h^{-2}$ ergs s^{-1}
L_B	$2.0 \times 10^{10} h^{-2} L_\odot$
M_{vir}^a	$(3.89^{+1.18}_{-3.10}) \times 10^{11} h^{-1} M_\odot$
M_{proj}	$(3.63^{+9.88}_{-2.23}) \times 10^{11} h^{-1} M_\odot$
M_{avg}	$(3.80^{+9.79}_{-2.13}) \times 10^{11} h^{-1} M_\odot$
M_{med}	$(3.09^{+3.76}_{-2.02}) \times 10^{11} h^{-1} M_\odot$
M_{tot}	$(3.63^{+5.41}_{-2.43}) \times 10^{11} h^{-1} M_\odot$
M_{tot}/L_B	$(18^{+27}_{-12}) h M_\odot / L_\odot$
M_{gal}	$(2.67 \pm 0.11) \times 10^{11} h^{-1} M_\odot$

^a Hickson et al. (1992) obtained a virial mass of SS, $M_{\text{vir}} = 1.38 \times 10^{11} M_\odot$, using $M_{\text{vir}} \simeq \pi V^2 R / 2G$, where V is the estimated intrinsic three-dimensional velocity dispersion, $V = [3(\langle v^2 \rangle - \langle v \rangle^2) - \langle \delta v^2 \rangle]^{1/2}$, v is the measured radial velocity of the galaxy, δv is the estimated velocity error, and $\langle \rangle$ denotes the average over all galaxies in the group, R is the median length of the two-dimensional galaxy-galaxy separation, G is the gravitational constant. In this study we estimated the virial mass of SS using the virial mass estimator taken from Heisler et al. (1985), $M_{\text{vir}} = [3\pi N \sum_i (v_i - \langle v \rangle)^2 / 2G \sum_{i < j} (1/R_{ij})]$, where N is the number of member galaxies, v_i is the radial velocity of the i -th galaxy, R_{ij} is the two-dimensional distance between the i -th galaxy and the j -th galaxy.

Next, we estimate the mass including dark matter associated with the member galaxies of SS, M_{gal} . The mean mass-to-luminosity ratios for each Hubble type are as follows: 13.7 ± 0.3 for early-type galaxies (Bacon, Monnet, & Simien 1985), and 9.1 ± 4.0 for Sdm galaxies, where we have estimated a typical mass-to-luminosity ratio for Sdm galaxies by averaging that of Sc galaxies, 5.2 ± 0.4 (Rubin et al. 1985), and that of irregular galaxies, 12.9 ± 7.5 (Lo, Sargent & Young 1993). Although HCG 79a and 79b are LINERs, the line emission has little effect on their B -band luminosities because the equivalent widths of H α emission, $EW(\text{H}\alpha)$, of these galaxies are less than several \AA (see Table 3). HCG 79d has a much larger $EW(\text{H}\alpha)$. However, its contribution to the total B -band luminosity of SS is only a few percent. Therefore, the B luminosity derived above can be regarded as the stellar B luminosity. We thus obtain an estimate of the total (i.e., stars, gas, and the dark matter) mass of the individual galaxies of SS, $M_{\text{gal}} \simeq 2.7 \times 10^{11} h^{-1} M_\odot$; note that M_{gal} does not contain the mass of dark matter in intragroup space. Since this mass is $73 \pm 3\%$ of the estimated dynamical mass of SS, it would appear that the majority of the dark matter may still be associated with the member galaxies. Since the dynamical mass measures the mass inside the circle enclosing the galaxies and is therefore insensitive to any mass outside it, we note that the ratio of 73% is an upper limit.

3.4. Dynamical Evolution of Seyfert's Sextet

We discuss the possible future evolution of SS. The irregular-shaped soft X-ray morphology of SS suggests that

TABLE 5
BASIC PROPERTIES OF THE ELLIPTICALS WITH LARGE-SCALE X-RAY HALO AND SS

Name	R (kpc)	M_{tot} (M_{\odot})	B_T^0 (mag.)	L_B (L_{\odot})	M_{tot}/L_B (M_{\odot}/L_{\odot})
SS	$8h^{-1}$	$3.63 \times 10^{11} h^{-1}$	12.94	$2.0 \times 10^{10} h^{-2}$	$18h$
RXJ 1340.6+4018	$170h^{-1}$	$1.4 \times 10^{13} h^{-1}$...	$3.7 \times 10^{10} h^{-2a}$	$373h$
NGC 1132	$243h^{-1}$	$1.9 \times 10^{13} h^{-1}$	13.03 ^b	$4.6 \times 10^{10} h^{-2}$	$413h$
NGC 4636	$300h^{-1}$	$9 \times 10^{12} h^{-1}$	10.43 ^b	$3.0 \times 10^{10} h^{-2}$	$297h$

^aEstimated from $M_{V_T} = -23.5$ (Ponman et al. 1994) with adopting $B - V = 1.04$ (Arimoto & Yoshii 1987) and $H_0 = 100h \text{ km s}^{-1} \text{ Mpc}^{-1}$.

^bTaken from de Vaucouleurs et al. (1991).

the dark matter in SS has not yet completely relaxed dynamically. This appears consistent with the following observations: 1) the member galaxies in SS show morphological and kinematic evidence for violent interactions, and 2) the majority of the dynamical mass of SS can be associated with the member galaxies. It is thus strongly suggested that SS is a dynamically-young, compact group of galaxies which will eventually merge. It has been numerically shown that the merging time scale of a compact group of galaxies, each member of which has a dark halo, is much shorter (i.e., $\sim 10^9 \text{ yr}$) than the Hubble time (Athanasoula, Makino, & Bosma 1998). Therefore, it is expected that SS will most likely merge into a single object within a time scale less than 10^9 years and finally evolve into an elliptical galaxy with a large, virialized halo. Such a fossil group of galaxies has been reported; a soft X-ray source RXJ 1340.6+4018 turns out to be an elliptical galaxy with a large-scale ($\sim 250 h^{-1} \text{ kpc}$) X-ray halo (Ponman et al. 1994; Jones et al. 2000). Other candidates may be the elliptical galaxy NGC 4636 in the Virgo cluster of galaxies (Matsushita et al. 1998) and an isolated elliptical galaxy NGC 1132 (Mulchaey & Zabludoff 1999).

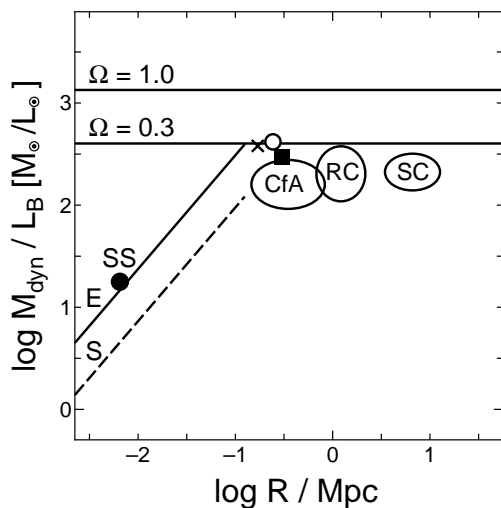


FIG. 8.— The relationship between the mass-to-optical B -band luminosity ratio and the size from Bahcall et al. (1995). The solid line and dashed line indicate the best fit lines for ellipticals and for spirals, respectively. The filled circle indicates SS. The open circle means NGC 1132. The filled square means NGC 4636. The cross indicates RXJ 1340.6+4018.

Finally, we investigate the relationship between the mass-to-light ratio (M_{tot}/L_B where L_B is the absolute B luminosity) and the radius (R) of SS and compare it with those of the candidate fossil groups and typical elliptical galaxies studied by Bahcall et al. (1995). The basic properties of the ellipticals with large-scale X-ray halos are listed in Table 5 taken from Ponman et al. (1994), Matsushita et al. (1998), and Mulchaey & Zabludoff (1999). Summing the blue luminosities of the four member galaxies, we obtain a total blue luminosity for SS, $L_{B,\text{tot}} \simeq 2.0 \times 10^{10} h^{-2} L_{\odot}$. We thus obtain a mass-to-light ratio for SS, $M/L_B \simeq 18h M_{\odot}/L_{\odot}$. The linear size of SS is $R \simeq 8h^{-1} \text{ kpc}$ which is the radius of a circle including the center of the four member galaxies. We also show these quantities in Table 5.

It seems worthwhile noting that the relationship between M/L_B and R for SS follows well that for elliptical galaxies (Bahcall et al. 1995; see Figure 4). We therefore suspect that the eventual merger remnant of SS may likely evolve into an ordinary elliptical galaxy.

We would like to thank an anonymous referee for his/her useful comments and suggestions. We would like to thank the staff members of the Okayama Astrophysical Observatory and the UH 2.2 m telescope for their kind assistance during our observations. We thank Harald Ebeling and Makoto Hattori for useful discussion on the X-ray data discussed in this paper. We also thank Richard Wainscoat and Shinki Oyabu for their kind help on photometric calibration and Youichi Ohya for his kind help during the course of this study. T. M. is supported by JSPS. This work was supported in part by the Ministry of Education, Science, Sports and Culture in Japan under Grant Nos. 07055044, 10044052, and 10304013.

REFERENCES

- Arimoto, N. & Yoshii, Y. 1987, *A&A*, 173, 23
 Athanassoula, E., Makino, J., & Bosma, A. 1998, *MNRAS*, 286, 825
 Bacon, R., Monnet, G., & Simien, F. 1985, *A&A*, 152, 315
 Bahcall, N. A., Lubin, L. M., & Dorman, V. 1995, *ApJ*, 447, L81
 Brown, B., & Bregman, J. N. 1998, *ApJ*, 495, L75
 de Vaucouleurs, G., de Vaucouleurs, A., Corwin, C. Jr., Buta, R. J., Paturel, G., & Fouqué, P. 1991, *Third Reference Catalogue of Bright Galaxies*. (Springer-Verlag)
 Ebeling, H., Voges, W., & Böhringer, H. 1994, *ApJ*, 436, 44

- Hamabe, M., & Ichikawa, S. 1992, in Proc. of Astronomical Data Analysis Software and Systems I, Astron. Soc. Pacific Conference Series, Vol. 25, eds. D. Worrall, Biemesderfer, and J. Barnes (ASP, San Francisco), 325
- Heisler, J., Tremaine, S., & Bahcall, J. N. 1985, ApJ, 298, 8
- Hickson, P. 1982, ApJ, 255, 382
- Hickson, P. 1993 Ap. Lett. Commun. 29, 1
- Hickson, P., Mendes de Oliveira, C., Huchra, J. P., & Palumbo G. G. C. 1992, ApJ, 399, 353
- Jewitt, D., Luu, J., & Chen, J. 1996, AJ, 112, 1225
- Jones, L. R., Ponman, T. J., & Forbes, D. A. 2000, MNRAS, 312, 139
- Kosugi, G., et al. 1995, PASP, 107, 474
- Landolt, A.U. 1992, AJ, 104, 340
- Lo, K. Y., Sargent, W. L. W., & Young, K. 1993, AJ, 106, 507
- Luppino, G., Metzger, M., Kaiser, N., Clowe, D., Gioia, I., & Mayazaki, S. 1996, in ASP Conf. Ser. 88, Clusters, Lensing, and the Future of the Universe, ed. V. Trimble & A. Reisenegger (San Francisco: ASP), 229
- Matsushita, K., Makishima, K., Ikebe, Y., Rokutanda, E., Yamasaki, N. Y., & Ohashi, T. 1998, ApJ, 499, L13
- Mendes de Oliveira, C., & Hickson, P. 1994, ApJ, 427, 684
- Mulchaey, J. S. & Zabludoff, A. I. 1998, ApJ, 496, 73
- Mulchaey, J. S. & Zabludoff, A. I. 1999, ApJ, 514, 133
- Nishiura, S. 1998, PhD Thesis, Tohoku University
- Nishiura, S., Shimada, M., Ohyama, Y., Murayama, T., & Taniguchi, Y. 2000, AJ, 120, No. 3. in press (astro-ph/0005281)
- Pildis, R. A., Bregman, J. N., & Evrard, A. E. 1995, ApJ, 443, 514
- Ponman, T. J., & Bertram, D. 1993, Nature, 363, 51
- Ponman, T. J., Allan, D. J., Jones, L. R., Merrifield, M., McHardy, I. M., Lehto, H. J., & Luppino, G. A. 1994, Nature, 369, 462
- Ponman, T. J., Bourner, P. D. J., Ebeling, H., & Böhringer, H. 1996, MNRAS, 283, 690 (P96)
- Read, A. M., Ponman, T. J., & Strickland, D. K. 1997, MNRAS, 286, 626
- Rubin, V. C., Burstein, D., Ford, W. K. Jr., & Thonnard, N. 1985, ApJ, 289, 81
- Rubin, V. C., Hunter, D. A., & Ford, W. K. Jr. 1991, ApJS, 76, 153
- Saracco, P., & Ciliegi, P. 1995, A&A, 301, 348
- Seyfert, C. K. 1948a, Phys. Rev., 74, 129
- Seyfert, C. K. 1948b, AJ, 53, 203
- Shimada, M., Ohyama, Y., Nishiura, S., Murayama, T., & Taniguchi, Y. 2000, AJ, 119, 2664
- Sulentic, J. W., & Lorre, J. J. 1983, A&A, 120, 36
- Vílchez, J. M., & Iglesias-Páramo, J. 1998, ApJS, 117, 1
- Vogler, A., Pietsch, W., & Kahabka, P. 1996, A&A, 305, 74
- Williams, B. A., McMahon, P. M., & van Gorkom, J. H. 1991, AJ, 101, 1957
- Worthey, G. 1994, ApJS, 95, 107

This figure "Nishiura_fig01.jpg" is available in "jpg" format from:

<http://arxiv.org/ps/astro-ph/0007220v1>

This figure "Nishiura_fig02.jpg" is available in "jpg" format from:

<http://arxiv.org/ps/astro-ph/0007220v1>

This figure "Nishiura_fig03.jpg" is available in "jpg" format from:

<http://arxiv.org/ps/astro-ph/0007220v1>

This figure "Nishiura_fig07.jpg" is available in "jpg" format from:

<http://arxiv.org/ps/astro-ph/0007220v1>